



1 Long-period solar annual and semiannual tidal contributions to the lowest
2 normal low water in seas surrounding China

3 Yanguang Fu¹, Dongxu Zhou¹, Yikai Feng¹, Xinghua Zhou^{1,2}

4 ¹ First Institute of Oceanography, Ministry of Natural Resources, Qingdao, Shandong, China

5 ² Shandong University of Science and Technology, Qingdao, Shandong, China

6

7 Abstract

8 As the chart datum of China, the lowest normal low water (LNLW) was calculated using three tidal
9 constituents, major (Q1, O1, P1, K1, N2, M2, S2 and K2), shallow water (M4, MS4 and M6) and
10 long-period tidal (Sa and Ssa). The construction of a tidal datum is mainly concerned with
11 improvements in the major tidal constituents, and the contribution of the long-period tidal
12 component has been generally neglected. In this study, long-term tide gauge observations and multi-
13 mission satellite altimetry data were used to investigate the spatial distribution of the long-period
14 tidal contribution in Chinese seas and analyze the relative long-period tidal contribution rate into
15 four regions. The results showed that the mean contribution in Chinese seas is 7.63%, with the
16 largest contribution in the Bohai Sea (11.33%) and smallest in the East China Sea (5.27%).
17 Differences between tide gauge and satellite-derived results were compared in detail. The Sa and
18 M2 tidal amplitudes are the main factors affecting the long-period tidal contribution to the LNLW.
19 The relative long-period tidal contribution can be up to 34.18% when tide gauge observations record
20 small M2 and large Sa amplitudes. These results indicate that the long-period tidal constituent
21 cannot be neglected in the establishment of the LNLW datum. Therefore, to improve tidal datum
22 precision, precise extraction and accuracy assessments of long-period tidal constituents should be a
23 research focus.

24 Keywords: tidal datum, chart datum, long-period tidal, lowest normal low water, China Sea

25

26 1. Introduction

27 The establishment of the surface of a chart datum is fundamental for accurate knowledge of
28 ocean depth (Gill et al., 2000). The lowest normal low water (LNLW) is the chart datum for the seas
29 around China and, as such, is important for safe navigation, maritime baseline determination and



30 vertical datums unification (Slobbe et al., 2018).

31 A chart datum is one type of tidal datum that can be derived from an average of low tidal
32 heights from sea level observations, or calculated by using tidal constituents extracted from tide
33 gauge measurements, satellite altimetry data and ocean tide models. Different types of tidal datums,
34 such as the lowest astronomical tide (LAT), mean lower low water (MLLW) and LNLW, have been
35 adopted as the chart datum in various countries to determine horizontal boundaries and provide
36 accurate vertical references for bathymetry (Wu et al., 2019).

37 Modern tidal datum model construction is based on an ocean tide model. The near continuous
38 digital expression is achieved through a high resolution grid, and the accuracy of the datum model
39 depends mainly on the tide model. For example, the US-based Vertical Datum Transformation
40 (VDatum) project used a regional ocean tide model to establish the MLLW surface (Parker et al.,
41 2003; Yang et al., 2010). The English Vertical Offshore Reference Frames (VORF) project produced
42 an inlaid tide model that combined a regional and global ocean tide model to establish a LAT model
43 (Ilfiffe et al., 2013). The advantage of the inlaid tidal model is that it improves the accuracy of diurnal
44 and semi-diurnal tidal constituents, but the LAT value does not include the effects of long-period
45 tidal constituents. In the global ocean tide model assessment (Cheng and Anderson, 2011; Carrere
46 et al., 2015; Egbert and Erofeeva, 2002), the accuracy performance of short-term tidal constituents
47 was analyzed in detail, but did not take into account long-period tidal constituents (Shum et al.,
48 1997; Stammer et al., 2014). Thus, there is a lack of accurate knowledge regarding long-period tidal
49 constituents.

50 Satellite altimetry data provide a continuous, high spatial resolution sea-level height time series
51 with near global coverage that allows for an accurate evaluation of the temporal–spatial
52 characteristics of long-period tidal constituents. However, satellite altimetry observations showed
53 poor accuracy performance, affected by land–sea interactions (Deng and Featherstone, 2006;
54 Gommenginger et al., 2011) and inaccurate geophysical correction models in coastal areas
55 (Andersen and Scharroo, 2011). In recent years, satellite altimetry has made great progress in
56 reducing instrument error and improving data processing and correction models (Passaro et al., 2014;
57 Verron et al., 2015; Pascual et al., 2015; Cotton et al., 2015), which makes it more feasible to obtain
58 a reasonable spatial distribution and reliable long-period tidal constituents. Handoko et al. (2017)
59 and Fu et al. (2020) carried out a detailed evaluation of the main geophysical corrections to derive
60 accurate sea surface heights in Indonesian seas and the South China Sea, respectively. As a result of



61 its current accuracy and maturity, altimetry is considered a fully operational observation system
62 dedicated to scientific and operational applications and more research is investigating the precision
63 of short-term tidal constituents (Fang et al., 2004; Zu et al., 2008; Victor et al., 2015; Cheng et al.,
64 2016). However, the contribution of long-period tidal constituents to the establishment of tidal
65 datums is still rarely studied (Yusof et al., 2017).

66 Long-period tides (e.g., 8 days, 2 weeks, 1 month, 6 months and 18.6 years) have been studied
67 since the time of Laplace. Wunsch (1967) reviewed the considerable late nineteenth and early
68 twentieth century analytical work by scientists such as Kelvin, Rayleigh, Poincaré and Proudman.
69 The long-period tidal correction, involving annual (Sa) and semi-annual (Ssa) tidal constituents, is
70 a component of the chart datum in China, but Sa and Ssa are not determined accurately. Most global
71 tide models do not provide long-period tidal constituents, except for FES2014 (Carrere et al., 2015)
72 and NAO99b (Matsumoto et al., 2000), but the long-period tidal constituents of those two models
73 only provide simulation results of pure fluid dynamics (amplitudes <1 cm). Thus, there is a large
74 difference with actual data obtained from tide gauge observations.

75 2. Data and methods

76 2.1 Tide gauge data

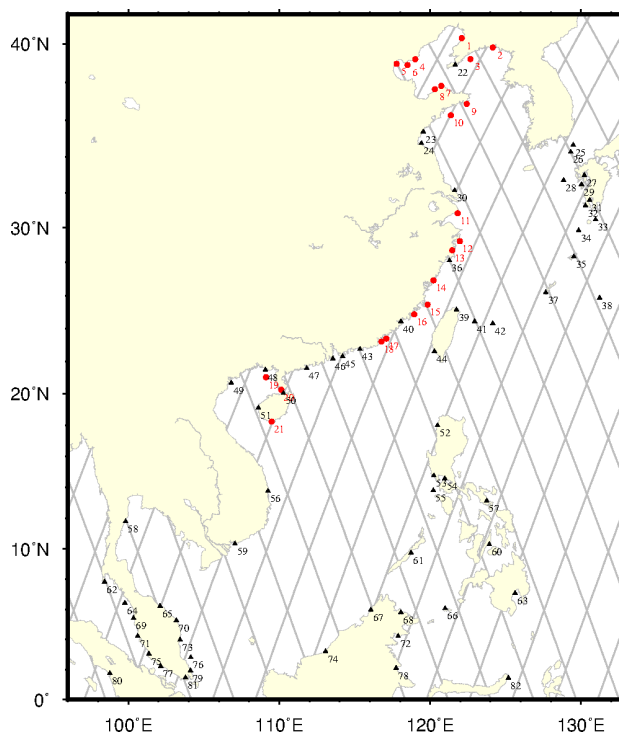
77 The harmonic constants of this study were obtained from 82 tide gauge observations, of which 61
78 stations were from the Tidal CONstants (TICON) data set (Piccioni, et al., 2019) and the other 21
79 stations were Chinese long-term tide gauge results (CLTR; Table 1, Figure 1).

80 TICON contains information on harmonic constants for 40 tidal constituents, derived from the
81 GESLA-2 tide gauge records (<http://www.gesla.org>) distributed on a quasi-global scale. The data
82 set is freely available from the PANGAEA repository ([https://doi.pangaea.de/10.1594/PANGA
83 EA.896587](https://doi.pangaea.de/10.1594/PANGAEA.896587)). The GESLA-2 tide gauge database contains 39,151 station years of data from 1355
84 stations (Woodworth et al., 2017). Most of these data were sampled hourly and the remainder more
85 frequently. For our analysis, the TICON and CLTR data sets were combined. The Chinese tide gauge
86 records had: 1) observation time series of at least a 3 year period and hourly value sampling, 2)
87 years with less than 85% of hourly values rejected, and 3) years for which the 3 year period was
88 centered on the middle of the year had less than 80% of hourly values rejected.

89 **Table 1.** Harmonic constants of annual (Sa) and semi-annual (Ssa) long-period tidal constituents collected from
90 Chinese tide gauge stations. The station locations are depicted in Figure 1.



Station No.	Name	Lon (deg)	Lat (deg)	Sa		Ssa	
				amp(cm)	pha(deg)	amp(cm)	pha(deg)
1	BYQ	122.10	40.30	29.12	201.39	2.89	32.40
2	CFD	118.51	38.92	27.52	203.63	3.18	344.52
3	CW	118.95	24.88	15.07	296.64	4.87	60.15
4	DG	124.15	39.82	27.55	207.66	3.21	28.94
5	HA	110.13	20.23	10.54	292.42	6.29	76.82
6	JJ	121.47	28.69	14.19	253.30	3.76	23.76
7	JTG	119.01	39.21	28.27	204.85	2.79	352.59
8	LK	120.32	37.65	25.12	209.95	1.47	331.86
9	LCG	121.83	30.83	19.77	227.49	2.52	6.50
10	NA	117.10	23.40	13.06	301.71	5.27	57.36
11	PL	120.74	37.83	24.82	210.42	1.39	346.74
12	PT	119.83	25.47	13.22	283.79	4.61	55.42
13	QLY	121.38	36.27	22.38	216.26	1.48	351.93
14	SS	120.22	26.92	13.61	274.62	4.38	57.26
15	SY	109.50	18.23	14.45	315.19	7.50	69.13
16	ST	116.78	23.22	13.00	302.15	5.67	59.45
17	SD	122.42	36.87	22.15	215.09	1.72	2.79
18	SP	121.97	29.22	16.55	244.01	2.69	38.39
19	TG	117.78	38.98	29.75	203.27	3.51	342.81
20	WZ	109.12	21.02	10.01	273.42	6.03	86.63
21	XCS	122.67	39.23	26.06	208.31	2.22	8.46



91

92 Figure 1. Tide gauge station distribution in the seas surrounding China. The red circles indicate Chinese long-
93 term tide gauge stations, while the black triangles are locations obtained from the Tidal Constants database. The
94 solid gray lines are the primary mission tracks.

95 2.2 Satellite altimetry data

96 We used satellite (TOPEX/Poseidon, Jason-1, Jason-2 and Jason-3) derived tidal constituent
97 data from February 1993 to May 2019. The 26 years long altimetric time series allows an analysis
98 of solar Sa and Ssa at a high level of precision.

99 The Center for Topographic Studies of the Ocean and Hydrosphere (CTOH;
100 <http://ctoh.legos.obs-mip.fr/>) is a French National Observation Service, supported by the Institut
101 National des Sciences de l'Univers, that conducts satellite altimetry studies. The CTOH provides
102 access to their frequently updated altimetric databases, including TOPEX/Poseidon, Jason-1, Jason-
103 2, GFO and ENVISAT data; they also provide access to altimetric products they develop. The sea
104 level anomaly time series has been computed for the TOPEX/Poseidon, Jason-1, Jason-2 and Jason-
105 3 data by applying the latest geophysical corrections. Tidal constants were then estimated directly
106 by harmonic analysis of each single time series from the along-track 1 Hz sea level anomalies. The



107 CTOH tidal constants contain along-track estimates of amplitude and phase for 43 tidal constituents
 108 (primary mission along-tracks in Figure 1).

109 2.3 Chart datum determination

110 A chart datum is usually related to the mean of low ocean surface, such as mean lower low
 111 water spring, mean low water, low water, LNLW or LAT, and various countries use different levels
 112 as the chart datum for their marine administration (Rahibulsadri, et al., 2014).

113 The LAT has been adopted as the chart datum where tides have an appreciable effect on the
 114 water level, as determined by the International Hydrographic Organization (International
 115 Hydrographic Bureau, 2010). LAT was defined as the lowest tide level that can be predicted to occur
 116 under average meteorological conditions and any combination of astronomical conditions. It was
 117 recommended that LAT be calculated either over a minimum period of 19 years using harmonic
 118 constants derived from an observation minimum of 1 year or by other methods known to give
 119 reliable results.

120 The LNLW has been adopted as the chart datum of China. LNLW was calculated with 13 tidal
 121 constituents, namely, diurnal and semi-diurnal (major; Q1, O1, P1, K1, N2, M2, S2 and K2), shallow
 122 water (M4, MS4 and M6) and long-period (Sa and Ssa; Marine Surveying and Mapping Institute of
 123 the PLA Navy, 1999):

$$124 \quad LNLW = L_8 + L_{shallow} + L_{long} \quad (1)$$

125 where $LNLW$ is the chart datum value. L_8 is the major tidal contribution, $L_{shallow}$ is the shallow water
 126 tidal contribution, and L_{long} is the long-period tidal contribution:

$$127 \quad \begin{aligned} L_8 = & R_{K_1} \cos \varphi_{K_1} + R_{K_2} \cos(2\varphi_{K_1} + 2g_{K_1} - 180^\circ - g_{K_2}) \\ & - \sqrt{(R_{M_2})^2 + (R_{O_1})^2 + 2R_{M_2}R_{O_1} \cos(\varphi_{K_1} + \alpha_1)} \\ & - \sqrt{(R_{S_2})^2 + (R_{P_1})^2 + 2R_{S_2}R_{P_1} \cos(\varphi_{K_1} + \alpha_2)} \\ & - \sqrt{(R_{N_2})^2 + (R_{Q_1})^2 + 2R_{N_2}R_{Q_1} \cos(\varphi_{K_1} + \alpha_3)} \end{aligned} \quad (2)$$

$$128 \quad L_{shallow} = R_{M_4} \cos \varphi_{M_4} + R_{MS_4} \cos \varphi_{MS_4} + R_{M_6} \cos \varphi_{M_6} \quad (3)$$

$$129 \quad L_{long} = R_{S_a} \cos \varphi_{S_a} + R_{S_{Sa}} \cos \varphi_{S_{Sa}} \quad (4)$$

130 where H and g are the amplitude and phase of each tidal constituent, respectively, f is the focus
 131 factor of each constituent, and $R = fH$. The LNLW is the one variable function of φ_{K_1} , which ranges
 132 from 0° to 360° . The minimum value of this function is the LNLW. According to the equilibrium
 133 relationship between tidal components, an approximate hypothesis was introduced:



$$\begin{aligned} \varphi_{M_4} &= 2\varphi_{M_2} + 2g_{M_2} - g_{M_4} \\ \varphi_{M_6} &= 3\varphi_{M_2} + 3g_{M_2} - g_{M_6} \end{aligned} \quad (5)$$

$$\begin{aligned} \varphi_{MS_4} &= \varphi_{M_2} + \varphi_{S_2} + g_{M_2} + g_{S_2} - g_{MS_4} \\ \varphi_{M_2} &= \tan^{-1} \left[\frac{(fH)_{O_1} \sin(\varphi_{K_1} + g_{K_1} + g_{O_1} - g_{M_2})}{(fH)_{M_2} + (fH)_{O_1} \cos(\varphi_{K_1} + g_{K_1} + g_{O_1} - g_{M_2})} \right] + 180^\circ \\ \varphi_{S_2} &= \tan^{-1} \left[\frac{(fH)_{P_1} \sin(\varphi_{K_1} + g_{K_1} + g_{P_1} - g_{S_2})}{(fH)_{S_2} + (fH)_{P_1} \cos(\varphi_{K_1} + g_{K_1} + g_{P_1} - g_{S_2})} \right] + 180^\circ \end{aligned} \quad (6)$$

$$\begin{aligned} \varphi_{Sa} &= \varphi_{K_1} - \frac{1}{2} \varepsilon_2 + g_{K_1} - \frac{1}{2} g_{S_2} - 180^\circ - g_{Sa} \\ \varphi_{Ssa} &= 2\varphi_{K_1} - \varepsilon_2 + 2g_{K_1} - g_{S_2} - g_{Ssa} \\ \varepsilon_2 &= \varphi_{S_2} - 180^\circ \end{aligned} \quad (7)$$

137 3. Regional variability in long-period tidal constituents

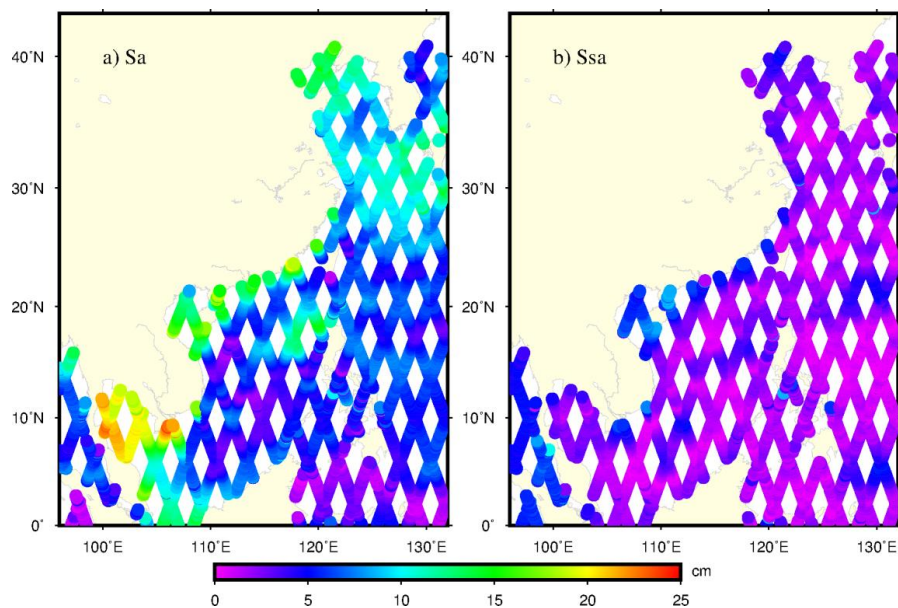
138 The spatial distribution of the satellite-derived along-track amplitude of Sa and Ssa is presented
 139 in Figure 2. The Sa maximum was 24.06 cm, with 79.1% of along-track points under 10 cm and
 140 63.9% in the range of 5–10 cm. The Ssa amplitude was smaller than Sa; the maximum amplitude
 141 was 10.29 cm, with 93.2% points under 5 cm. We observed that the long-period tidal amplitude
 142 showed a gradual change along the spatial gradient, with smaller magnitudes in the deep open ocean
 143 and maximum values distributed in the Gulf of Thailand (Figure 2). The accuracy of the satellite-
 144 derived long-period tidal data depends, to some extent, on the sea level time series duration of the
 145 ascending and descending orbital. Our data indicate that the satellite-derived long-period tidal
 146 constituents present high internal accuracy, which can be mainly attributed to the long time series
 147 (>25 years; February 1993 to May 2019).

148 The maximum, minimum and mean amplitude values of satellite-derived Sa and Ssa are listed
 149 in Table 2. The seas around China were divided into four regions: the Bohai Sea (38–41°N, 119–
 150 127°E), the Yellow Sea (33–38°N, 117–126°E), the East China Sea (23–33°N, 117–131°E), and the
 151 South China Sea (0–23°N, 100–122°E). Different sub-oceans have different numbers of along-track
 152 satellite points. For example, for 153 along-track points in the Bohai Sea, the Sa and Ssa average
 153 values were the largest in this study (Sa = 9.47–17.91 cm; Ssa = 1.74–5.85 cm). Overall, there were
 154 400, 1298 and 4224 along-track points in the Yellow Sea, East China Sea and South China Sea,
 155 respectively.

156 In general, the satellite-derived long-period tidal constituents presented large spatial



157 differences and gradual spatial gradients, which suggest that they contribute to spatial variability in
 158 the chart datum.



159
 160 Figure 2. Satellite-derived tidal amplitudes of annual (Sa) and semi-annual (Ssa) long-period tidal constituents.

161 **Table 2.** Amplitude of satellite-derived annual (Sa) and semi-annual (Ssa) long-period tidal constituents in
 162 different seas (cm).

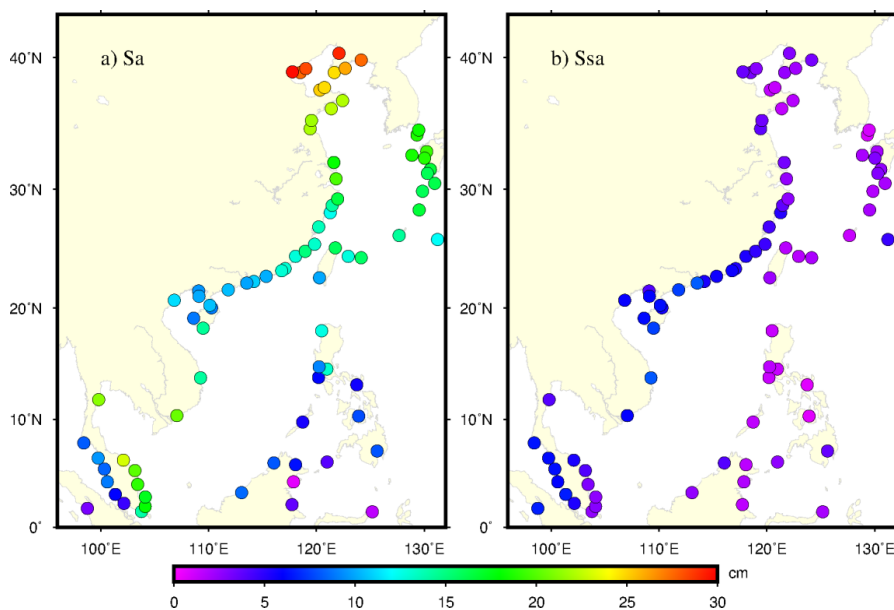
Sea area	Sa			Ssa		
	min	max	average	min	max	average
Bohai Sea	9.47	17.91	12.65	1.74	5.85	3.31
Yellow Sea	6.19	14.63	9.29	0.10	4.28	1.76
East China Sea	2.46	19.88	8.65	0.04	9.16	1.68
South China Sea	0.28	24.06	8.09	0.03	9.91	2.17

163 Long-term tide gauge stations provide highly accurate and high resolution tidal height values.
 164 In recent studies, tide gauge results have been regarded as true data to ground truth satellite-derived
 165 or tide model results. Our 18.61 year time series was ideal to obtain true tidal constituents because
 166 there is a relationship between longer durations of tide level data collection and higher tidal
 167 constituent precision. At least one full year of tide gauge observations is required to obtain Sa values,
 168 although this may include large inaccuracies in the data. To ignore the effects from different tide



169 scales, we obtained Sa and Ssa from 82 long-term tide gauge stations (Figure 3).

170 Compared with the satellite-derived results, the amplitude of Sa varied over a larger scale
171 (0.64–29.75 cm). However, the amplitude of Ssa was more restricted (0.67–8.16 cm). The large
172 difference in Sa and Ssa is mainly a result of their behavior in the Bohai Sea.



173

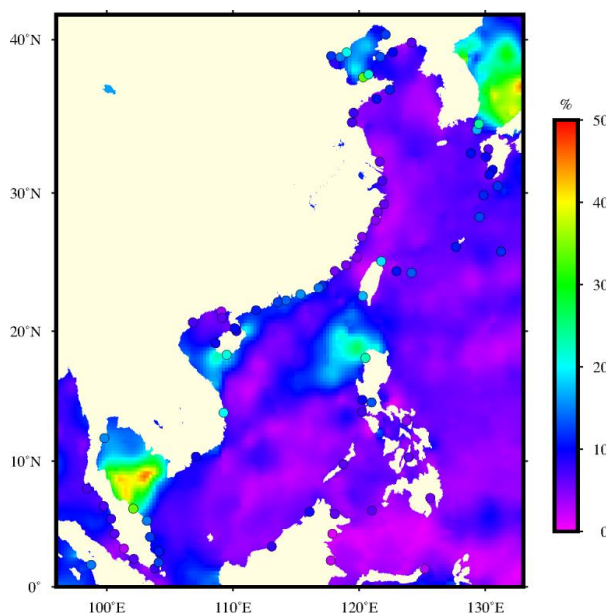
174

Figure 3. Amplitude of Sa and Ssa tidal in the long-term tide gauge stations.

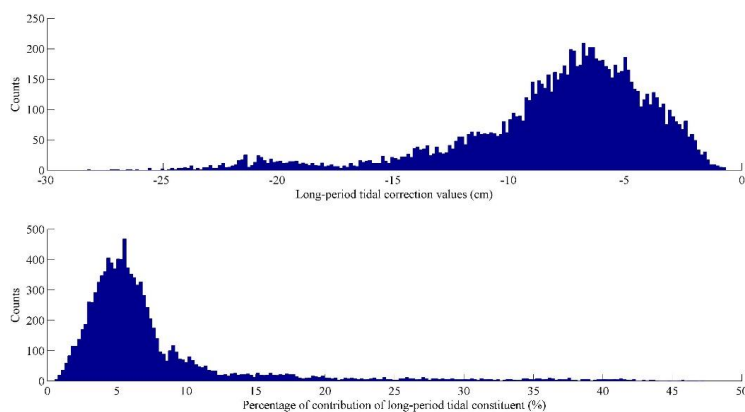
175 4. Magnitude of tidal contributions to tidal datum

176 The long-period tidal correction values and contributions were calculated for each satellite
177 along-track point using Eq. (1). The relative long-period tidal contribution refers to the percentage
178 of long-period tidal corrections in the LNLW.

179 The satellite-derived results were interpolated onto a $15' \times 15'$ grid by using the anti-distance
180 weighted method. The maximum long-period tidal contributions were found in the Gulf of Thailand,
181 the northeastern South China Sea and Japan Sea (Figure 4). Overall, 74.0% of the along-track long-
182 period tidal contribution values were in the range of -20 to -5 cm, 3.0% were under -20 cm and 23.3%
183 were above -5 cm; the average value was 7.48% (Figure 5).



184
185 Figure 4. Spatial distribution of satellite-derived long-period tidal contributions. The dots depict results from tidal
186 gauge stations.



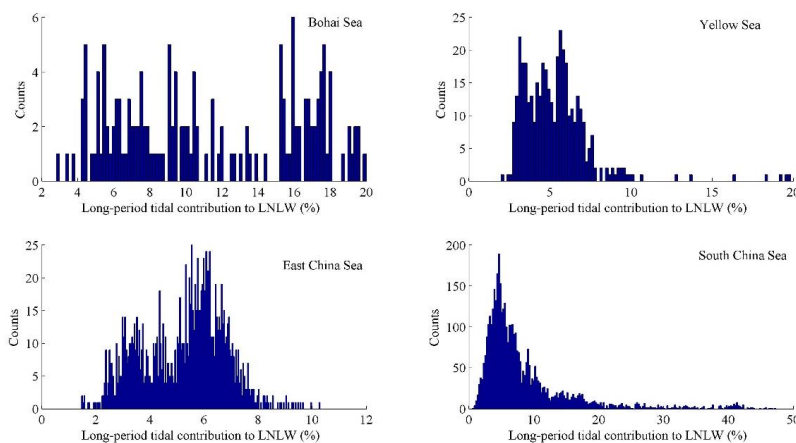
187
188 Figure 5. Histograms of the long-period tidal correction values and contribution.

189 To investigate the relative (%) performance of long-period tidal contributions in Chinese seas,
190 histograms of the contributions were plotted for each of the four regions (Figure 6) with results
191 listed in Table 3. In the Bohai Sea, about 52% of along-track points were above 10% and 92% of
192 the contributions were above 5%; the average value was 20%. Additionally, the average long-period
193 tidal contribution value was -13.58 cm. The long-period tidal contributions were remarkable in this



194 area, mainly because of the large amplitude for Sa. In the Yellow Sea, East China Sea and the South
 195 China Sea, the relative contributions above 5% were 52%, 62% and 63%, respectively. Some of the
 196 variation among the regions is also a result of the different numbers of along-track points in the
 197 different ocean basins.

198 There are three types of tidal constituents, major (diurnal and semi-diurnal), shallow water and
 199 long-period, used to establish the LNLW. Our data showed that these three types have different
 200 relative contributions in the seas surrounding China. The long-period contribution exceeded 5% in
 201 all regions, with maximum values (11.33%) in the Bohai Sea and the South China Sea (8.56%). The
 202 overall relative long-period tidal contribution was 7.63%.



203
 204 Figure 6. Distribution of the long-period tidal constituent contributions to lowest normal low water (LNLW).

205 **Table 3.** Relative contribution (%) of the individual tidal constituents to the lowest normal low water (LNLW).

Sea area	Major tidal contribution	Shallow water tidal contribution	Long-period tidal contribution
Bohai Sea	86.59	2.08	11.33
Yellow Sea	91.63	3.01	5.35
East China Sea	93.68	1.04	5.27
South China Sea	89.71	1.73	8.56

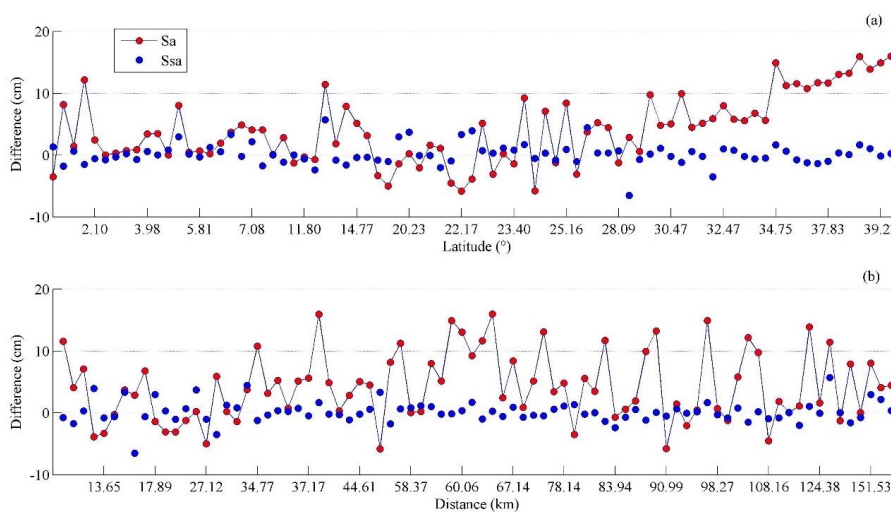
206 **5. Discussion**

207 The long-period tidal constituent amplitude is the main cause of differences in the tidal
 208 contributions. An accuracy assessment of the satellite-derived long-period tidal constituents was



209 carried out by comparing results from the 82 tide gauge stations with the nearest satellite along-
210 track point. The difference in Sa amplitude was between -5.84 cm and 15.99 cm, and 81.7% of Sa
211 values were under 10 cm (average = 4.20 cm; standard deviation = 5.57 cm). The difference in Ssa
212 amplitude was between -6.54 cm and 5.69 cm, with 84.1% of values ± 2 cm (average = 0.16 cm;
213 standard deviation = 1.72 cm).

214 We can see that differences in Sa amplitudes were larger in the higher latitude areas (Figure
215 7a); for example, the amplitude difference ranged from 4.47 cm to 9.94 cm in 29.22–34.65°N and
216 10.76–15.99 cm north of 34.75°N. These results indicate that amplitude differences are bigger in
217 the tide gauge data than satellite-derived results. Figure 7b shows the amplitude difference as a
218 function of distance between a tide gauge station and the nearest satellite along-track point.
219 Distances ranged from 1.93 km to 164.08 km, although a significant correlation between them was
220 not found. Overall, 87% of positions that had amplitude differences of ± 10 cm had <60 km between
221 a satellite point and tide gauge station; for distances >60 km, the relevant percentage between ± 10
222 cm decreased to 77%. These results also confirm that long-period tidal constituents have a wide
223 spatial scale.



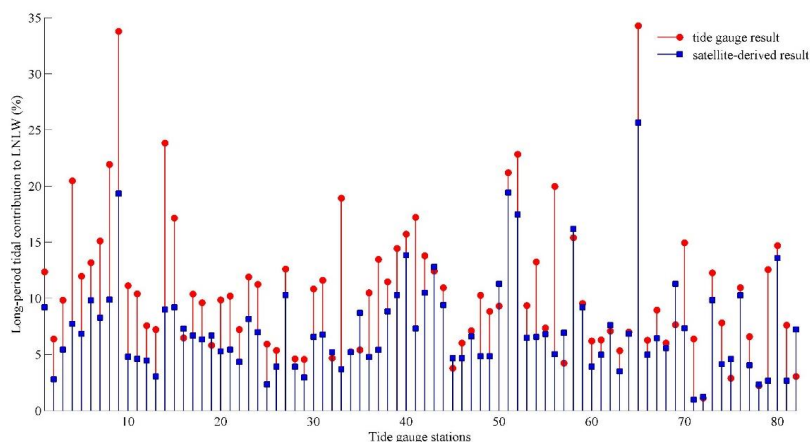
224
225 Figure 7. Relationship of annual (Sa) and semi-annual (Ssa) tidal component amplitude differences and (a) the
226 latitudes of tide gauge stations, and (b) the distance between a tide gauge station and the nearest satellite along-
227 track point.

228 Furthermore, the data processing strategy can be another important source of error between



229 tide gauge data and satellite-derived results. As the long-period tidal constituent can be affected by
230 atmospheric factors, particularly barometric pressure, the inverse barometric correction is one of the
231 main factors needed to obtain long-period tidal information. Because the target chart datum
232 investigated here is mainly used in navigation safety, our aim was to provide a conservative ocean
233 depth; thus, we have not carried out inverse barometric corrections on the tide gauge data.

234 Figure 8 shows a comparison of relative long-period tidal contributions from tide gauge data
235 and satellite-derived results. The difference between them ranges from -4.20% to 15.27%, with 35.3%
236 of stations within $\pm 2\%$, and 74.4% of stations within $\pm 5\%$. The maximum relative contribution
237 was 34.18% (station No. 65, see Figure 1) and the second highest was found in the Yellow Sea
238 (station No. 8, 33.78%). Station No. 8 had a Sa amplitude of 25.12 cm; however, this was not the
239 largest amplitude compared with surrounding stations. For example, station No. 5 showed the largest
240 amplitude (29.75 cm), with long-period tidal correction values of -25.24 cm and -27.22 cm, but a
241 relative long-period tidal contribution of only 11.98%. Actually, the amplitude values at stations No.
242 8 and No. 5 were mainly influenced by the amplitude of short-period tidal constituents, especially
243 the M2 tidal component. As the largest source of diurnal and semi-diurnal tidal components, the M2
244 amplitude at stations No. 5 and No. 8 station were 27.56 cm and 102.92 cm, respectively. Major
245 tidal correction values were -112.09 cm (No. 5) and -241.93 cm (No. 8), which resulted in large
246 differences between the relative long-period tidal contribution.



247

248 Figure 8. Latitudinal (x-axis) comparison of long-period tidal contributions from tide gauge data. Tide gauge
249 station locations are in Figure 1.



250 **6. Conclusions**

251 Tide gauge and satellite altimetry data were used to study the long-period tidal contribution of
252 the Sa and Ssa tidal constituents to the LNLW in seas surrounding China. The LNLW was calculated
253 using 13 different tidal constituents (Q1, O1, P1, K1, N2, M2, S2, K2, M4, MS4, M6, Sa and Ssa).
254 A long-period tidal correction was carried out by combining the Sa and Ssa tidal constituents.

255 The satellite-derived along-track Sa and Ssa amplitudes were 24.06 cm and 10.29 cm,
256 respectively. The maximum long-period tidal correction and relative contribution was -28.26 cm
257 (mean = -7.97 cm) and 47.2% (mean = 7.48%), respectively. The mean relative long-period tidal
258 contribution was largest in the Bohai Sea (11.33%) and smallest in the East China Sea (5.27%); this
259 parameter was affected by the total number of along-track points in the different regions. The Sa
260 amplitude obtained from 82 long-term tide gauge stations was between 0.64 cm and 29.75 cm, and
261 the Ssa was between 0.67 cm and 8.16 cm. The low precision of satellite altimetry data in coastal
262 areas and tidal height data processing are the main factors that contributed to differences between
263 tide gauge data and satellite-derived results. A determination of the effect of inverse barometric
264 corrections on the extraction of long-period tidal constituents will be necessary in subsequent studies.
265 The reasons for differences in the relative long-period tidal contributions between tide gauge data
266 and satellite-derived results were analyzed. Long-period tide corrections result from Sa and Ssa tidal
267 component data, but were affected by the small amplitude of Ssa and influenced by the Sa amplitude.
268 The amplitude of M2 tidal values was found to be another important factor affecting the long-period
269 tidal contribution. The overall relative long-period tidal contribution in the four studied regions was
270 7.63%, but it was up to 34.18% at some tide gauge stations. The long-period tidal correction is vital
271 to the establishment of the LNLW, and a precise extraction and accuracy assessment of long-period
272 tidal constituents will be the focus of future research.

273

274 **Acknowledgments**

275 Satellite altimetry data used in this study were developed, validated, and distributed by the
276 CTOH/LEGOS, France. The authors would like to acknowledge the CTOH for providing the
277 satellite-derived harmonic constants of tidal constituents, TICON data set provide the harmonic
278 constants.



279 Reference

- 280 Andersen OB, Scharroo R. 2011. Range and geophysical corrections in coastal regions: and
281 implications for mean sea surface determination. In Coastal Altimetry, edited by S. Vignudelli,
282 A. Kostianoy, P. Cipollini and J. Benveniste, chap.5 . Springer-Verlag.
- 283 Carrere L, Lyard F, Cancet M, et al. 2015. FES 2014, a new tidal model on the global ocean with
284 enhanced accuracy in shallow seas and in the Arctic region. Geophysical Research Abstracts.
- 285 Cheng YC, Anderson OB. 2011. Multimission empirical ocean tide modeling for shallow waters
286 and polar seas. *Journal of Geophysical Research*, 116, C11001.
- 287 Cheng YC, Xu Q, Zhang Y. 2016. Tidal estimation from TOPEX/Poseidon, Jason primary, and
288 interleaved missions in the Bohai, Yellow, and East China Seas. *Journal of Coastal Research*,
289 2016, 32(4): 966–973.
- 290 Deng X, Featherstone W. 2006. A coastal retracking system for satellite radar altimeter waveforms:
291 application to ERS-2 around Australia. *Journal of Geophysical Research*, C06012.
- 292 Egbert GD, Erofeeva SY. 2002. Efficient inverse modeling of barotropic ocean tides. *Journal of*
293 *Atmospheric and Oceanic Technology*, 19: 183–204.
- 294 Fang G, Wang Y, Wei Z, et al. 2004. Empirical cotidal charts of the Bohai, Yellow, and East China
295 Seas from 10 years of TOPEX/Poseidon altimetry. *Journal of Geophysical Research*, 109:
296 C11006.
- 297 Fu Y, Zhou D, Zhou X, et al. 2020. Evaluation of satellite-derived tidal constituents in the South
298 China Sea by adopting the most suitable geophysical correction models. *Journal of*
299 *Oceanography*, 76: 183-196. doi:10.1007/s10872-019-00537-2
- 300 Gill, S.; Schultz, J. *Tidal Datums and Their Applications*; NOAA Special Publication NOS CO-OPS
301 1: Silver Spring, MD, USA, 2000. Available online:
302 http://www.tidesandcurrents.noaa.gov/publications/tidal_datums_and_their_applications.pdf
303 (accessed on 6 February 2019).
- 304 Gommenginger C, Thibaut P, Fenoglio-Marc L, et al. 2011. Retracking altimeter waveforms near
305 the coasts. In Coastal Altimetry, edited by S. Vignudelli, A. Kostianoy, P. Cipollini and J.
306 Benveniste, chap. 4 . Springer-Verlag.
- 307 Handoko EY, Fernandes MJ, Lázaro C. 2017. Assessment of altimetric range and geophysical



- 308 corrections and mean sea surface models—impacts on sea level variability around the
309 Indonesian seas. *Remote Sens-Basel*, 9: 102.
- 310 Iliffe JC, Ziebart MK, Turner JF, et al. 2013. Accuracy of vertical datum surfaces in coastal and
311 offshore zones. *Survey Review*, 45(331): 254–262.
- 312 International Hydrographic Bureau (2010) Resolutions of the international hydrographic
313 organization, Publication M-3 2nd edn.
- 314 Marine Surveying and Mapping Institute of the PLA Navy. 1999. Specifications for hydrographic
315 survey. GB 12327-1998. Beijing: Standards Press of China.
- 316 Matsumoto K, Takanezawa T, Masatsugu O. Ocean tide models developed by assimilating
317 TOPEX/POSEIDON altimeter data into hydrodynamical model: a global model and a regional
318 model around Japan. *Journal of Oceanography*, 2000, 56: 567-581.
- 319 Piccioni Gaia, Dettmering Denise, Bosch Wolfgang, Seitz Florian. TICON: Tidal CONstants based
320 on GESLA sea-level records from globally located tide gauges. *Geoscience Data Journal*, 2019,
321 00: 1–8. DOI: 10.1002/gdj3.72
- 322 Parker B, Milbert D, Hess K, et al. 2003. National VDatum-the implementation of a national Vertical
323 Datum Transformation database. *Sea Technology*, 44(9): 10–15.
- 324 Rasheila Rahibulsadri, Abdullah Hisam Omar, Ashraf Abdullah, Wan Muhammad Aizzat Wan
325 Azhar, Hasan Jamil, Teng Chee Hua, Chan Keat Lim and Tan Ah Bah. Determination of Tidal
326 Datum for Delineation of Littoral Zone for Marine Cadastre in Malaysia. *Geoinformation for
327 Informed Decisions*, 2014, 219-230, DOI: 10.1007/978-3-319-03644-1_16.
- 328 Shum CK, Woodworth PL, Andersen OB, et al. 1997. Accuracy assessment of recent ocean tide
329 models. *Journal of Geophysical Research: Oceans*, 102 (C11): 25173–25194.
- 330 Slobbe DC, Sumihar J, Frederikse T, et al. 2018. A Kalman filter approach to realize the lowest
331 astronomical tide surface. *Marine Geodesy*, 41: 44–67.
- 332 Stammer D, Ray RD, Andersen OB, et al. 2014. Accuracy assessment of global barotropic ocean
333 tide models. *Review of Geophysical*, 52 (3): 243–282.
- 334 Victor BD, Rosa C, Oliveira D, et al. 2015. Extraction of tide constituents by harmonic analysis
335 using altimetry satellite data in the Brazilian coast. *Journal of Atmospheric and Oceanic
336 Technology*, 32 (3): 614–626.



- 337 Woodworth, P. L., Hunter, J. R., Marcos, M., Caldwell, P., Menéndez, M., and Haigh, I.: Towards a
338 global higher frequency sea level dataset. *Geoscience Data Journal*, 3: 50–59,
339 <https://doi.org/10.1002/gdj3.42>, 2017.
- 340 Wu W., Myers E., Shi L., et al., 2019. Modeling Tidal Datums and Spatially Varying Uncertainty in
341 the Texas and Western Louisiana Coastal Waters. *Journal of Marine Science and Engineering*,
342 7,44. Doi: 10.3390/jmse7020044
- 343 Wunsch C. 1967. The long-period tides. *Reviews of Geophysics*. 5(4): 447-475.
- 344 Yang Z, Myers E, White S. 2010. VDatum for eastern Louisiana and Mississippi coastal waters:
345 tidal datums, marine grids, and sea surface topography. NOAA Technical Memorandum, NOS
346 CS 19.
- 347 Yusof N, Mahmud M, Abdullah M. 2017. Effect of long term tidal constituents on mean sea level
348 trend during El-Nino and La-Nina phenomena. *The International Archives of the*
349 *Photogrammetry, Remote Sensing and Spatial Information Sciences*, Volume XLII-4/W5, 2017
350 GGT 2017, 4 October 2017, Kuala Lumpur, Malaysia.
- 351 Zu T, Gan J, Erofeeva SY. 2008. Numerical study of the tide and tidal dynamics in the South China
352 Sea. *Deep-Sea Research*, 55(2): 137–154.